JOURNAL OF VIROLOGY, Apr. 2000, p. 3804–3814 Vol. 74, No. 8
0022-538X/00/$04.00+0

A Beta-Stranded Motif Drives Capsid Protein Oligomers of the Parvovirus Minute Virus of Mice into the Nucleus for Viral Assembly

ELEUTERIO LOMBARDO,[1]† JUAN C. RAMÍREZ,[1]† MAVIS AGBANDJE-MCKENNA,[2] AND JOSÉ M. ALMENDRAL[1]*

Centro de Biología Molecular "Severo Ochoa" (Consejo Superior de Investigaciones Científicas—Universidad Autónoma de Madrid), 28049 Cantoblanco, Madrid, Spain,[1] and Department of Biological Sciences, University of Warwick, Coventry CV4 7AL, United Kingdom[2]

Received 18 October 1999/Accepted 3 January 2000

The determinants of nuclear import in the VP-1 and VP-2 capsid proteins of the parvovirus minute virus of mice strain i (MVMi) synthesized in human fibroblasts were sought by genetic analysis in an infectious plasmid. Immunofluorescence of transfected cells revealed that the two proteins were involved in cooperative cytoplasmic interactions for nuclear cotransport. However, while VP-1 translocated regardless of extension of deletions and did not form capsid epitopes by itself, VP-2 seemed to require cytoplasmic folding and the overall conformation for nuclear transport. The sequence $_{528}$KGKLTMRAKLR$_{538}$ was found necessary for nuclear uptake of VP-2, even though it was not sufficient to confer a nuclear localization capacity on a heterologous protein. In the icosahaedral MVMi capsid, this sequence forms the carboxy end of the amphipathic beta-strand I (βI), and all its basic residues are contiguously positioned at the face that in the unassembled subunit would be exposed to solvent. Mutations in singly expressed VP-2 that either decrease the net basic charge of the exposed face (K530N-R534T), perturb the hydrophobicity of the opposite face (L531E), or distort the βI conformation (G529P) produced cytoplasmic subviral oligomers. Particle formation by βI mutants indicated that the basic residues clustered at one face of βI drive VP oligomers into the nucleus preceding and uncoupled to assembly and that the nuclear environment is required for MVMi capsid formation in the infected cell. The degree of VP-1/VP-2 transport cooperativity suggests that VP trimers are the morphogenetic intermediates translocating through the nuclear pore. The results support a model in which nuclear transport signaling preserves the VP-1/VP-2 stoichiometry necessary for efficient intranuclear assembly and in which the beta-stranded VP-2 nuclear localization motif contributes to the quality control of viral morphogenesis.

The successful multiplication of many viruses depends on their gaining access to the transcription and replication machineries confined in the nucleus of the eukaryotic cell. Viruses of different compositions and sizes enter the nucleus during their life cycles in the form of particles, complexes, or virion subunits (28). These viruses use molecular interactions connecting to the physiological nuclear transport pathways of the cellular proteins. In the eukaryotic cell, most karyophilic polypeptides actively transported through the nuclear pore complex (NPC) (65) harbor a nuclear localization signal (NLS) necessary for nuclear import. In the so-called classical form, the NLS consists of a short sequence of basic amino acids either in a single cluster, as originally described for the simian virus 40 large T antigen (33), or in two domains, as for the nucleoplasmin bipartite nuclear targeting sequence (51). The import pathway of classical NLS-bearing proteins into the nucleus proceeds by consecutive interactions comprising importins α and β (14, 15; reviewed in reference 42), and additional soluble factors to dock to the cytoplasmic periphery of the NPC (60) and to move across its central gated channel (50). However, an increasing number of alternative nuclear transport pathways operate by nonclassical NLS which do not fit a consensus and bind different families of import receptors (38, 46). For example, the nuclear targeting sequence of the heterogeneous nuclear ribonucleoprotein (hnRNP) A1 protein is a segment of 40 amino acids (the M9 domain) rich in glycines and aromatic residues that uses a receptor termed transportin (47), for the hnRNP K protein the signal is an unrelated long sequence (the KNS domain) that accesses a distinct import pathway (40), and the ribosomal proteins carry more than one functional nuclear import signal of greater complexity than the classical NLS (57) that can recognize receptors from classical and nonclassical pathways (29, 54).

The nuclear translocation of viral polypeptides also operates via NLSs similar to the ones described for cellular proteins. Classical and nonclassical NLSs are found in DNA viruses irrespective of the complexity of their genomes (35), as well as in those RNA viruses that use the nucleus for their multiplication (72). Moreover, the interaction of virus polypeptides with components of the nuclear import machinery (34, 43) plays crucial roles in viral tropism and host range (48, 71). Hence, the domains and receptors used by viruses to invade the nucleus offer new targets for interfering with their multiplication and for improving the technology of gene delivery.

Parvoviridae is a family of single-stranded nonenveloped DNA viruses that replicate and mature in the nucleus of proliferative cells (4, 17), and some of its members are highly pathogenic for animals and humans. The structure at atomic resolution for the T=1 icosahaedral capsid of several parvoviruses have been determined using X-ray crystallography (1, 68, 74). The major capsid protein VP-2 has an eight-stranded

* Corresponding author. Mailing address: Centro de Biología Molecular "Severo Ochoa" (CSIC-UAM), Universidad Autónoma de Madrid, 28049 Cantoblanco, Madrid, Spain. Phone: 34-91-3978048. Fax: 34-91-3978087. E-mail: JMAlmendral@cbm.uam.es.

† Present address: Centro Nacional de Biotecnología (CSIC), 28049 Cantoblanco, Madrid, Spain.

antiparallel β-barrel topology formed by β-strands B to I, commonly found in small viral capsids (53), and four prominent loops that confer the surface biological properties of the capsid such as host range determinants (3, 44) and antigenic sites (5, 45). Several steps of parvovirus morphogenesis, for example the step involving the subcellular compartment where the capsid is primarily formed, are poorly understood. Although the capsids of adeno-associated virus (AAV) are first detected in the nuclei of infected cells (26, 73), it is unclear if the 25-nm parvovirus capsid, which is at the size limit of particles traversing the NPC (19), may pass through it at a postassembly stage prior to nuclear accumulation. Assignment of the nuclear transport sequence in the capsid proteins should help clarify the parvovirus assembly pathway.

We have sought the determinants of translocation through the NPC in the structural proteins of the strain i of the autonomous parvovirus minute virus of mice (MVMi) (7), an important mouse pathogen and a reference molecular model for this viral family. MVMi infects neuroblasts, lymphoid cells, and other cellular types in developing organs of lethally inoculated newborn mice (9, 49) and dysregulates the hematopoiesis of immunodeficient mice (59). The MVMi genome is organized as two transcriptional units regulated by *cis*- and *trans*-acting signals (see Fig. 1A). The capsid is composed of two polypeptides at the ratio of synthesis, with the larger, VP-1 (83 kDa), being expressed from two exons and the smaller, VP-2 (64 kDa), contained in the second exon of VP-1, so that the two proteins are identical in amino acid sequence except for the first 142 residues of the VP-1 N terminus (66). Both VP-1 and VP-2 reach the nucleus when transfected alone, but only VP-2 is capable of forming capsids that encapsidate virus progeny DNA, while VP-1 is necessary for infectivity (69). This report provides new insights into the functions played by the capsid proteins in MVMi life cycle. We show that VP-1 and VP-2 cooperate in nuclear transport by undergoing cytoplasmic in vivo interaction, but in spite of their sequence identity, they differ in folding capacity in the infected cell, as well as in the sequence necessary for independent nuclear translocation. Furthermore, a novel nuclear localization motif in a beta-strand of VP-2 plays a major role in MVMi morphogenesis and may help us understand the regulation of the nuclear transport process by signals affecting protein conformation.

MATERIALS AND METHODS

Cell lines. The human simian virus 40-transformed fibroblast cell line NB324K, permissive for MVMi productive infection (22), was used for the nuclear transport study, and COS-7 cells were used for the analysis of protein expression in blots. A clone of NB324K cells was selected by plaque assay for maximal susceptibility to MVMi infection to improve reliability in the immunofluorescence (IF) assays. Cells were cultured in Dulbecco modified Eagle medium (DMEM; Gibco BRL) supplemented with 5% heat-inactivated fetal calf serum (FCS) (Bio Whittaker).

Construction of deletion mutants in the MVMi capsid proteins. In order that the phenotypes of the VP mutants could be regarded in the context of the natural MVMi infection, all the mutants analyzed in this work were constructed in an infectious plasmid (pMVMi [22]), kindly provided by P. Tattersall (Yale University, New Haven, Conn.). Plasmid constructs were transformed and amplified in *Escherichia coli* JC8111 (a gift from C. R. Astell, University of British Columbia, Vancouver, Canada), a strain that permits deletion-resistant propagation of MVM plasmid clones bearing terminal palindromes (6). Mutants with deletions at precise amino acid positions of the common sequence of VP-1 and VP-2 proteins (Fig. 1B) were constructed based on technical constraints imposed by the availability of restriction sites. The Δ60–90 mutation was generated using the single *Spe*I site at MVM position 3000 (2). Plasmid pMVMi was cut at this site and digested with nuclease *Bal* 31 (1 unit/μg of DNA; Boehringer Mannheim) and ligated, and an in-frame mutation was selected by DNA sequencing. The Δ98–127, Δ138–267, Δ161–225, and Δ174–231 mutants were constructed by subcloning the pMVMi *Hin*dIII-*Xba*I fragment in the pUC19 plasmid, cutting it at the *Nco*I (nucleotide [nt] 3125) and *Pst*I (nt 3365) sites, and serially digesting it with *Bal* 31 nuclease as described for Δ60–90. In-frame mutants were subcloned like a *Hin*dIII-*Xba*I fragment in pMVMi. Δ218–322 was obtained by cutting the same pUC19-derived plasmid at the *Hin*dII sites (nt 3445 and 3760) and self-ligated, and the *Hin*dIII-*Xba*I fragment was inserted into pMVMi as above. Δ323–473 was made using the *Bgl*II site of pMVMi (nt 3450), filling the restriction site with Klenow polymerase, digesting with *Hpa*I at its single site (nt 3760), and religating it to yield the in-frame deletion. The Δ218–473 mutant was obtained by total digestion at the two *Bgl*II sites (nt 3450 and 4210) of pMVMi and self-ligation. Δ474–517 was constructed by cutting the pMVMi plasmid at the *Bgl*II (nt 4210) and *Xba*I (nt 4345) sites and filling in the ends with Klenow to generate an in-frame junction. Δ519–587 was generated using the *Xba*I site and filling in with Klenow polymerase, creating a frameshift which disrupts the VP open reading frame and introduces a single Lys-518–to–Ser change and an amber stop codon at position 519.

A mutant without the VP-1 protein (ΔVP-1/wt plasmid) was obtained by cutting pMVMi at the *Hin*dIII site, digesting it with nuclease *Bal* 31, and isolating a mutant harboring the nt 2590 to 2710 deletion, which introduces a frameshift in the VP-1 open reading frame joining the peptide DHLLTFL to the first 74 amino acids of the VP-1 N-terminus and then an ochre stop codon at nt 2733. The ΔVP-1/Δ161–225, ΔVP-1/Δ174–231, ΔVP-1/Δ323–473, ΔVP-1/Δ474–517, and ΔVP-1/Δ519–587 mutants with deletions in both VP-1 and the indicated VP-1/VP-2 common region (Fig. 1E) were constructed by exchanging the *Xho*I-*Spe*I fragment (nt 2073 to 3000) of the corresponding deletion mutant with the equivalent fragment of the ΔVP-1/wt plasmid. The expression and respective sizes of the deleted VP proteins were probed by immunoblot analysis of transfected COS-7 cells (data not shown).

Site-directed mutants. Mutations were introduced by oligonucleotide-directed mutagenesis by the procedure described by Kunkel (36), using the M13mp18 phage vector, and were transferred to the MVMi genome by exchanging the *Xba*I-*Ssp*I fragment (nt 4345 to 4630) of either the wild-type (wt) or the ΔVP-1/VP-2wt plasmid for the mutated fragment. The amino acid and nucleotide changes, numbered from the start of VP-2, and their position in the virus genome, respectively, were as follows: Lys-530 to Asn (K530N), A-4384 to T; Arg-534 to Thr (R534T), G-4395 to C; Gly-529 to Pro (G529P), GG-4379, 4380 to CC; Leu-531 to Glu (L531E), CT4385, 4386 to GA; Met-533 to Glu (M533E), AT-4391, 4392 to GA; Met-533 to Phe (M533F), AG-4391, 4393 to TT; and Thr-532 to Arg (T532R), C-4389 to G. The amino acid stretch KGKLTM RAKLR, corresponding to the nuclear localization motif of VP-2, was inserted in frame with the bacterial β-galactosidase protein by cloning the CCAAAGG AAAACTAACAATGAGAGCAAAGCTTAGA oligonucleotide and its complementary strand into the *Kpn*I restriction site (nt 204) of plasmid pCH110 (Pharmacia). Mutants were sequenced by the dideoxy-mediated chain termination method incorporating [^{35}S]dATP with T7 DNA polymerase (Pharmacia) and were verified in the double-stranded plasmid DNA preparations to be used for cell transfection. Sequencing and mutagenic oligonucleotides were purchased from Isogen Bioscience BV (Maarssen, The Netherlands).

Transfection. NB324K and COS-7 cells were transfected either by lipofection or by electroporation with plasmid preparations enriched in supercoiled forms by either CsCl gradient equilibrium centrifugation or chromatography through Qiaprep columns (Qiagen). For electroporation, 1.5×10^6 cells in 0.1 ml of cooled DMEM supplemented with 4% FCS were added to 10 μg of plasmid and 25 μg of carrier salmon sperm DNA and immediately electroporated by applying one pulse at 230 V and 250 μF for NB324K and 200 V and 960 μF for COS-7 in a Gene Pulser apparatus with capacitance extender (Bio-Rad). Cells were diluted in DMEM supplemented with 5% FCS and seeded at a density of 1.5×10^6 cells per 35-mm dish, and the medium was replaced after 16 h. For liposome-mediated transfection, 12 μg of plasmid DNA was incubated for 15 min at room temperature with 60 μl of Lipofectin transfection reagent (Gibco BRL) in a total volume of 550 μl of DMEM without antibiotics. The mixture was diluted with 1.6 ml of the same medium and added to monolayers of washed serum-free cells that had been seeded at 2.5×10^5 cells per 60-mm dish 24 h previously. After a 6-h incubation, DMEM supplemented with 10% FCS was added up to 6 ml, left for 16 h, and replaced with new DMEM–5% FCS.

Preparation of antisera. The peptide MAPPAKRAKRGWC, corresponding to the first 12 amino acid residues of the unique N-terminal region of VP-1 plus an extra cysteine residue (2), was synthesized on an Applied Biosystems model 431A peptide synthesizer by standard Fast Moc chemistry and purified by reverse-phase high-pressure liquid chromatography. The synthetic peptide was activated and covalently conjugated in excess molar ratio to keyhole limpet hemocyanin (Pierce) with heterobifunctional cross-linker *m*-maleimidobenzoyl-*N*-hydroxysuccinimide ester by standard methods (23). The conjugate was extensively dialyzed against phosphate-buffered saline (PBS) and used to raise an antiserum in 8-week-old BALB/c female mice by intraperitoneal injection of each mouse with a 50-μg dose of conjugate emulsified in Freund's complete adjuvant followed by three boost injections in incomplete adjuvant. The specificity of the antiserum for VP-1 was demonstrated by immunoblotting MVMi-infected NB324K cells. A capsid polyclonal antiserum against MVM purified empty particles raised in a rabbit has been previously described (56). Hybridoma culture producers of anti-MVM capsid monoclonal antibodies (MAb), prepared and supplied by C. Parrish (Cornell, Ithaca, N.Y.), were grown in DMEM supplemented with 20% FCS. The supernatant fluids to be used in IF were tested for titer and specificity by a conventional enzyme-linked immunosorbent assay against native or heat-denatured purified MVM capsid as antigen. The exclusive reactivity of the MAbs with intact MVM capsid and not with subviral complexes

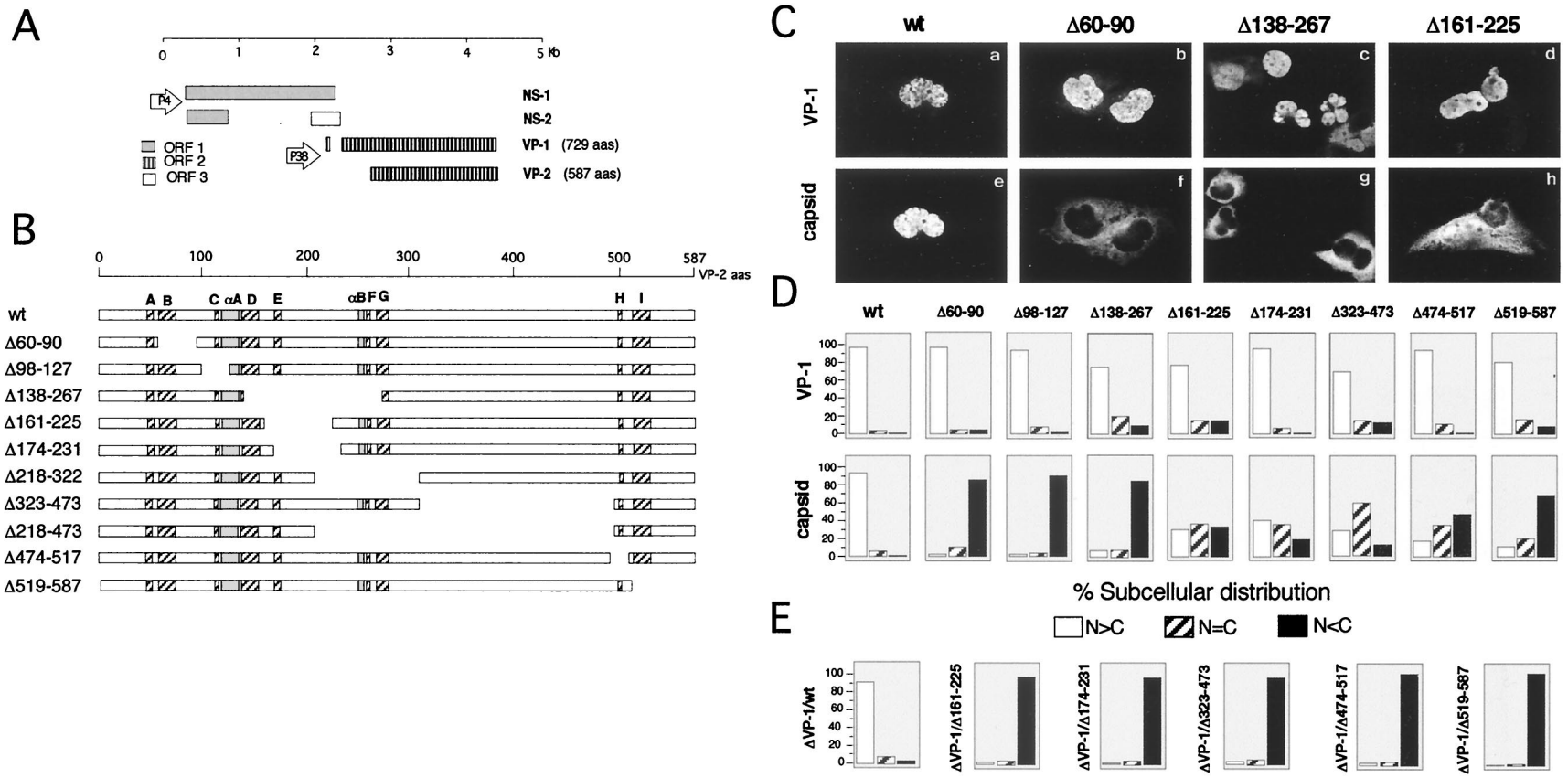

FIG. 1. The capsid proteins of MVMi cooperatively interact in the cytoplasm for nuclear import. (A) MVMi genetic organization. Virus genes are expressed from two promoters (arrows), P4, driving the expression of the nonstructural proteins (NS-1 and NS-2), and P38, driving the expression of the structural proteins (VP-1 and VP-2). The coding sequences of these proteins are depicted as boxes at the respective reading frames (based on reference 17). For simplicity, the three NS-2 isoforms that result from alternate minor splicing patterns have been omitted. (B) Collection of deletion mutants constructed in the VP-1/VP-2 common region of the MVMi genome. The 587-amino-acid stretch of the VP-2 sequence is shown as an open box, including the main stretches with ordered secondary structure in the MVMi three-dimensional capsid (1): βA to βI (hatched boxes) and α-helices αA and αB (shaded boxes). Numerals indicate the corresponding VP-2 residues flanking the deletions. (C) Diversity of phenotypes found in the MVMi capsid deletion mutants. Upper panels: (a, b, and d) nuclear VP-1 labeling; (c) cells showing some cytoplasmic VP-1 staining. Lower panels: capsid staining in the nucleus (e), cytoplasm (f and g), and nucleus and cytoplasm (h). The same field of cells is shown for both antigens, except in panels c and g of the Δ138–267 mutant. (D) Subcellular distribution of VP antigens in the deletion mutants. The values are the average percentage from at least 300 IF-positive cells counted in the 24- to 40-h posttransfection period from two independent experiments. Scored cells were classified in three categories: IF staining mostly nuclear (N>C), comparable nuclear and cytoplasmic staining (N=C), and staining mainly cytoplasmic (N<C). (E) Subcellular localization of VP-2 in deletion mutants deprived of VP-1 (ΔVP-1). Data are expressed as the percentage of transfected cells with a characteristic phenotype for the subcellular distribution of VP-2 ($n > 200$).

was further probed by the analysis of their reactivity against VP subunits and capsids fractionated in sucrose gradients (results not shown).

Indirect immunofluorescence. Cells were seeded onto glass coverslips at a density of 1.0×10^6 cells per 35-mm dish, and 24 to 40 h posttransfection the monolayers were washed twice with PBS and fixed in methanol-acetone (1:1) at −20°C for 7 min. Air-dried cells were then studied by double-label indirect IF with primary and secondary (Jackson ImmunoResearch Laboratories, Inc.) antibodies diluted 1:100 in PBS supplemented with 5% horse serum and incubated for 45 min each at room temperature. Bound immunoglobulin G was visualized with a goat anti-rabbit antibody conjugated to Texas red or with a goat anti-mouse antibody conjugated to fluorescein isothiocyanate. The intracellular localization of β-galactosidase in transfected cells was determined with a specific MAb (Zymed Laboratories, Inc.). Samples were dehydrated with ethanol and mounted in Mowiol. Cells were viewed by epifluorescence with a Zeiss Axiophot microscope at a magnification of ×400, and images were photographed with TMAX 400 film (Kodak).

Sedimentation analysis in sucrose gradients. NB324K cultures were labeled from 24 to 40 h posttransfection with 250 μCi of [^{35}S]methionine-[^{35}S]cysteine (Pro-mix; Amersham) per ml in methionine-free DMEM–10% dialyzed FCS supplemented with 10% normal medium. The cells were harvested by being washed twice with cold PBS, and the monolayer was scraped into TNEM buffer (150 mM NaCl, 50 mM Tris [pH 8.0], 1 mM EDTA, 2 mM $MgCl_2$) plus inhibitors (1 μg of leupeptin per ml, 1 μg of pepstatin per ml, 1 μg of aprotinin per ml, 1 mM phenylmethylsulfonyl fluoride) and disrupted in a cooled water bath sonicator. Cellular lysates were clarified by centrifugation at 15,000 × *g* and 4°C for 30 min in a bench-top centrifuge. Extracts from 2×10^6 transfected cells in 0.5 ml were layered onto 12 ml of a continuous 5 to 30% sucrose gradient in TNEM buffer prepared on ice, and ultracentrifuged at 160,000 × *g* in an SW40 rotor (Beckman) at 5°C for 4 h, and 0.6-ml fractions were collected from the top. Bovine serum albumin (67 kDa; 4.3S), thyroglobulin (670 kDa; 19S), MVMi empty capsids (70S), and DNA-full virions (110S) highly purified on density gradients were used as molecular size markers in the gradients. The distribution of the protein standards in the gradient fractions was visualized by Coomassie blue staining of reducing sodium dodecyl sulfate (SDS)-containing gels and of the MVMi particles by hemagglutination. For immunoprecipitation, 250 μl of each fraction was adjusted to 150 mM NaCl, 50 mM Tris (pH 8.0), and 1% Nonidet P-40 with inhibitors as above and incubated overnight at 4°C with rabbit anti-MVM capsid antiserum. Immune complexes were precipitated with protein A-Sepharose (10%, wt/vol) and washed with cold PBS–0.05% Nonidet P-40–1% bovine serum albumin. Bound proteins were eluted by heating the samples for 5 min at 95°C in Laemmli buffer and subjected to SDS-polyacrylamide gel electrophoresis (10% polyacrylamide). Purified ^{35}S-labeled virus was loaded onto the gels to identify the VP-2 protein. The gels were fixed, dried, and exposed for autoradiography. Images were obtained by a 48-h exposure in a phosphorimager (BAS1000; Fujix).

Molecular computer graphics. The molecular computer graphics analysis of the VP-2 G529P mutant was conducted with coordinates of the MVMi capsid protein deposited in the Brookhaven database (accession no. 1MVM), using the interactive computer graphics program O (31) on a Silicon Graphics Indigo 2 workstation. Possible disruption of the beta-strand I (βI) configuration due to this mutation was examined by interactive mutation in O followed by refinement constrained with standard geometry in the O database and inspection of the resultant βI conformation.

RESULTS

The VP-1 and VP-2 capsid proteins of parvovirus MVMi differ in their sequence requirements for nuclear transport. For a preliminary examination of the sequences involved in the nuclear transport of the VP-1 and VP-2 capsid proteins of MVMi, a series of in-frame truncation mutations were made in the VP gene of an infectious plasmid, expanding the region encoding the polypeptide sequence common to both proteins (Fig. 1B). The VP deletion mutants were individually transfected into human fibroblast NB324K cells, and the structural proteins were localized in the cells by double indirect IF 24 to 40 h afterwards. The VP-1 and capsid antigens colocalized in the nucleus of cells transfected with the wild-type infectious MVMi plasmid (Fig. 1C, panels a and e), but their subcellular distribution differed in all the deletion mutants and was generally opposite. The specific immunoreactivity of VP-1 was mostly nuclear for all the mutants tested (Fig. 1C and D), including Δ218–322 and Δ218–473 (results not shown). Thus, VP-1 translocated to the nucleus regardless of structural rearrangements generated by the large deletions. In contrast, a predominant nuclear localization of the capsid antigen was never observed for any of the VP deletion mutants. Mutants Δ60–90, Δ98–127, and Δ138–267 showed cytoplasmic capsid localization as the major phenotype (Fig. 1C, panels b and c, and 1D), while all the other mutants (Δ161–225, Δ174–231, Δ323–473, Δ474–517, or Δ519–587) showed a mixture of nuclear and cytoplasmic phenotypes. For mutants Δ218–322 and Δ218–473, anticapsid reactivity was not seen in repeated transfection trials (data not shown), presumably due to their lack of immunodominant epitopes mapped at amino acid 232 to 322 (5, 12, 44).

The antiserum raised against purified MVMi empty capsids failed to recognize the larger VP-1 protein, as it could be clearly evidenced in cells transfected with several mutants. For example, in transfections with the Δ60–90 mutant (Fig. 1C, panels b and f), the VP-1 N-terminal anti-peptide antibody showed that VP-1 was localized exclusively in the nucleus while capsid immunoreactivity was only cytoplasmic. This observation suggested that the capsid antiserum immunoreacted with conformational epitopes that could be formed by wt and mutant VP-2 proteins, but not the VP-1 protein, upon folding, either as a monomer or as supramolecular assembly intermediates, consistent with the previously described differential capacities of VP-1 and VP-2 to form capsids when transfected alone (69). Thus, the capsid antibody traces only the subcellular distribution of VP-2. The phenotypes of the mutants shown in Fig. 1D indicated that, unlike VP-1, VP-2 nuclear transport was hampered by all the deletions constructed in the VP gene.

The nuclear translocation of VP-2 can be modulated by cytoplasmic interaction with VP-1. The VP-2 mixed subcellular distribution found in deletion mutants Δ161–225, Δ174–231, Δ323–473, Δ474–517, and Δ519–587 under an efficient nuclear accumulation of VP-1 (Fig. 1D) suggested that a cytoplasmic interaction of VP subunits could influence the IF phenotypes. To examine this hypothesis and to quantitatively determine the contribution of VP-1 cooperativity to VP-2 nuclear import, these mutants were genetically deprived of VP-1 (see Materials and Methods) and upon transfection the cells were probed for independent VP-2 subcellular distribution (Fig. 1E). In the absence of VP-1, the wt VP-2 protein translocated to the nucleus with an efficiency comparable to that found in the wt infectious MVMi plasmid (Fig. 1E, ΔVP-1/wt). However, the deleted VP-2 protein remained predominantly in the cytoplasm in all the ΔVP-1 deletion mutant derivatives analyzed (Fig. 1E, ΔVP-1/Δ161–225, ΔVP-1/Δ174–231, ΔVP-1/Δ323–473, ΔVP-1/Δ474–517, and ΔVP-1/Δ519–587). Taking these data together, two conclusions can be drawn. First, VP-1 shows an efficient cooperative activity in the nuclear translocation of VP-2, and second, every deletion in the VP gene determines an absolute cytoplasmic retention of the singly expressed VP-2. These results indicated an extreme sensitivity of VP-2 nuclear transport to deletions in any part of its sequence and suggested that this VP-2 protein capacity is driven by a sequence(s) whose function depends on the folding status of the polypeptide region common to both structural proteins.

The sequence targeting MVMi VP-2 capsid protein to the nucleus functions under a β-strand configuration. A search for NLSs along VP-2 revealed one single region enriched in basic amino acids lying within the sequence $_{528}$KGKLTMRAKLR$_{538}$ near the C terminus of the protein. This sequence does not conform any consensus NLS, since it lacks the two or more contiguous basic residues found in all the classical NLSs (21) and in most of the characterized nonclassical sequences with nuclear localization activity (38, 40, 72). In the crystal structure of the mature MVMi icosahaedral capsid (1), this sequence forms the carboxy half of the βI strand (residues 520 to 538 of VP-2) of the eight-stranded antiparallel β-barrel, and

it is disposed at the inner capsid surface (Fig. 2A). Interestingly, all the βI basic amino acids are positioned at the face of the strand exposed to the solvent and are not involved in capsid subunits contacts, while most of the uncharged and hydrophobic residues occur on the other face, giving a marked amphipathic character to this strand (Fig. 2B, top). The sensitivity of VP-2 nuclear transport to genetic deletions and the capacity of VP-2 to fold, exposing immune system-recognizable capsid epitopes in the cytoplasm (see above), prompted the investigation of the hypothesis that the basic sequence within βI is the NLS of VP-2 functioning in the precise conformation observed in the capsid structure.

To determine the role of the βI sequence in VP-2 uptake into the nucleus, site-directed mutagenesis was used to exchange the most exposed basic amino acids of βI in an MVMi plasmid genome with the VP-1 coding region deleted (mutant ΔVP-1/VP-2wt) for evolutionarily conserved but uncharged residues (8, 67). The single mutation R534T had no significant effect on the subcellular localization of the VP-2 protein, but cells transfected with the double site-directed mutant ΔVP-1/VP-2 K530N–R534T showed a predominant retention of the VP-2 protein in the cytoplasm (Fig. 2B). However, the exchange of residue types at positions T532 and R534 (mutant ΔVP-1/VP-2 T532R-R534T) and of residue types at positions K530 and T532 (mutant ΔVP-1/VP-2 K530T-T532K) did not alter the phenotype of the mutant VP-2 proteins with respect to the wt protein (Fig. 2B). Therefore, whereas classical NLSs are sensitive to point mutations at specific critical residues (33), the sequence necessary for VP-2 nuclear transport in MVMi remains functional regardless of the internal rearrangements of residues within βI, which do not alter its net basic charge. In support of the notion that the VP-2 nuclear localization capacity harbored by βI is distinct from classical linear NLSs, which are commonly sufficient to confer affinity for the nuclear compartment to a heterologous protein (32), the entire K528–R538 sequence inserted in frame into the bacterial β-galactosidase enzyme (see Materials and Methods) was unable to affect the cytoplasmic localization of this protein (data not shown).

The role of the face of βI not exposed to solvent in VP-2 nuclear uptake was explored by using a second series of mutations which most likely distort the configuration of the amphipathic βI strand while preserving the basic charges (Fig. 2B, lower part). Mutation of a glycine residue (G529) located in the middle of βI, where the strand has a natural twist, to a proline (mutant ΔVP-1/VP-2 G529P) completely retained the mutant VP-2 protein in the cytoplasm to the extent that no cells showed nuclear staining. Molecular graphics computer modelling of the possible effects of this mutation on βI configuration, using the coordinates of the available crystal structure of MVMi virions (see Materials and Methods), indicated that this mutation is highly likely to cause disruption of βI topology as a result of a steric clash between the inserted Pro ring and the side chain of W527 (data not shown). Mutations of the L531 or both the L531 and M533 uncharged residues, with a high intrinsic β-sheet-forming propensity (41) to glutamic acid (mutants ΔVP-1/VP-2 L531E and ΔVP-1/VP-2 L531E-M533E), which is known to be poor at forming β-sheets (63), also resulted in an absolute retention of VP-2 in the cytoplasm (Fig. 2B). An increased local acidity at this face of the strand possibly prevented the configuration of βI, thereby abolishing its nuclear translocation capability. Mutating M533 to the bulkier phenylalanine (mutant ΔVP-1/VP-2 M533F) in the internal face of βI determined a cytoplasmic retention of VP-2 slightly greater than that observed for the wt protein. In combination, the mutational analysis indicated that the basic nature of the exposed face of βI, as well as the hydrophobic contacts mediated by the residues on the interior face, played key roles in the VP-2 protein nuclear translocation process. Thus, the amphipathic basic charge and hydrophobic distribution of the residues on the two faces of βI, which can be configured only upon VP-2 protein folding, appears to be essential for its functionality. This sequence in βI, which functions not in a linear form but under a precise conformation, is hereafter referred to as the VP-2 nuclear localization motif (NLM).

The VP-2 NLM drives nuclear translocation of VP oligomers for subsequent capsid assembly. The uncertainty of the compartment in which parvovirus MVM capsid assembly initiates leaves open the possibility that βI configuration is necessary for VP-2 protein folding and assembly in the cytoplasm, prior to translocation of this small capsid through the NPC. If this is the correct course of events, the NLM mutants would halt nuclear transport by precluding capsid assembly. To assign the function of the NLM of VP-2 in the assembly pathway of MVMi capsid, we studied the capacity of VP-2 mutants to oligomerize into supramolecular complexes by sedimentation analysis through sucrose gradients and to form capsids in the nucleus and in the cytoplasm.

The wt VP-2 protein (mutant ΔVP-1/VP-2wt) produced oligomers of approximately 4S to 10S at the upper fractions of the gradient, as well as high-molecular-weight complexes sedimenting in the range expected for empty capsids and virions (Fig. 3A, wt), in agreement with the reported capacity of this protein to form DNA-full particles when expressed alone (69). Mutant M533F, competent for nuclear transport (Fig. 2B), gave a sedimentation pattern similar to that of the wt protein. In contrast, this pattern was severely altered in the two other mutants tested (ΔVP-1/VP-2 K530N-R534T and ΔVP-1/VP-2 G529P), which had shown a predominantly cytoplasmic phenotype for VP-2 (Fig. 2B). The VP-2 subunits of the K530N-R534T double mutant also formed mainly oligomers in the upper fractions of the gradient, together with a small proportion of particles sedimenting as empty capsids (70S) demonstrable in overexposed gels (Fig. 3A), although here DNA-full virion (110S) formation was not seen. Preliminary analysis of the ordered DNA in the interior of the MVMi capsid (1) indicates that residue R534 of VP-2 interacts by hydrogen bonding with base N21 (data not shown), and thus its disruption may cause the failure of recognition and encapsidation of the MVMi genome. Finally, the single-change G529P mutation retained VP-2 subunits at the upper fractions, with no evidence of particle formation (Fig. 3A, bottom). These experiments indicated that a functional NLM may be dispensable for the stable oligomerization of VP-2 protein subunits, but it is required for efficient capsid formation.

Most cells transfected with the infectious wt MVMi plasmid showed nuclear staining with polyclonal antiserum (Pas) and with an anti-capsid specific MAb (Fig. 3B, panels a and g), but cells showing a mixed or cytoplasmic phenotype for the Pas were respectively only nuclear or negative for MAb reactivity (Fig. 3B, panels b and h and diagram to the right). In transfections with the ΔVP-1/VP-2 K530N-R534T double mutant, only the low proportion of cells with nuclear phenotype for the Pas showed anti-capsid MAb staining in the nucleus, although most cells had a major cytoplasmic phenotype (Fig. 3B, panels c and j). Consistently, every cell within the high percentage showing a cytoplasmic phenotype with the Pas was negative for MAb immunoreactivity regardless of its fluorescence intensity (Fig. 3B, panels d and j and diagram to the right). Therefore, the K530N-R534T VP-2 protein does not form capsids in the cytoplasm, even though it harbors an inherent capacity to ef-

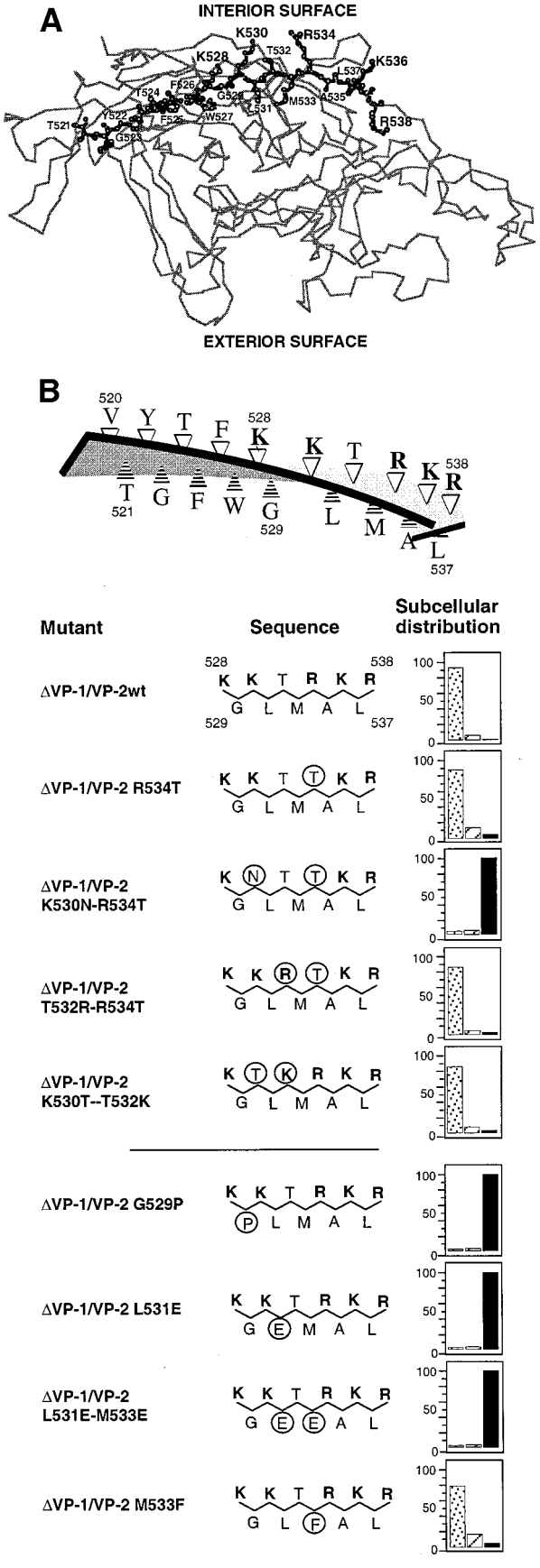

FIG. 2. A beta-strand configuration of βI is the determinant for VP-2 nuclear transport. (A) Location of βI in an unassembled VP-2 subunit. The βI is highlighted, with the basic side chains facing outward to the solvent. Basic charged amino acids are shown in bold. The figure was produced by the program Molview (64) from available coordinates (PDB, accession no. 1MVM). (B) The VP-2 NLM. (Upper) VP-2 NLM as disposed on βI. (Lower) Phenotypes of mutants engineered at the exposed face (top five) or at the hydrophobic face (bottom four) of βI. The target amino acids of VP-2 subjected to mutational analysis are circled, and basic amino acids are shown in bold. Transfected cells were phenotypically characterized for VP-2 subcellular distribution with an MVM capsid antiserum and classified into the three categories illustrated by the diagrams: stippled bar, nuclear phenotypes; striped bar, mixed phenotypes; black bar, cytoplasmic phenotypes. Similar percentages were obtained at 24 or 40 h post-transfection ($n > 200$ per mutant). Single-letter code for the amino acids: A, Ala; E, Glu; F, Phe; G, Gly; K, Lys; L, Leu; M, Met; P, Pro; R, Arg; T, Thr, W, Try; Y, Tyr.

ficiently assemble into capsids, as demonstrated in the few cells in which it targets the nucleus. When this VP-2 mutant protein was coexpressed with VP-1 (mutant VP-1/VP-2 K530N-R534T), while VP-1 targeted the nucleus of most cells (Fig. 1C and D), the nuclear localization of VP-2 was remarkably increased by the cooperative VP-1 interaction, up to around 50% of the transfected cells (Fig. 3B, bottom). Immunoprecipitation from fractionated ^{35}S-labelled transfected cells showed that the percentage of cells for each phenotype was a good reflection of the average VP-2 protein subcellular distribution (data not shown). However, most transfected cells were negative for the MAb reactivity irrespective of their phenotype for the Pas (Fig. 3B, panels e to l, and corresponding bars to the right), indicating that the large accumulation of VP-1 and VP-2 protein subunits at a nonphysiological stoichiometry in the nuclear compartment did not lead to capsid formation. These results dissociated the process of nuclear transport of viral structural proteins from the assembly of MVMi capsid and collectively demonstrated that a functional NLM in βI is required for translocation of VP oligomers into the nucleus, allowing capsid assembly to occur.

DISCUSSION

The two capsid proteins of parvovirus MVMi translocate to the nucleus by using different sequences and protein conformational requirements. The study reports the molecular mechanisms regulating the nuclear translocation of the parvovirus MVMi VP-1 and VP-2 capsid proteins synthesized in permissive transformed human cells. A series of contiguous and overlapping deletion mutants of various lengths were constructed in the VP gene of an infectious MVMi plasmid to map sequences with nuclear localization capacity. In spite of their amino acid identity (with the entire VP-2 sequence being included in VP-1), these proteins translocate to the nucleus using different mechanisms with respect to the amino acid domains involved and the requirements of specific protein conformations in the overlapping region. The larger VP-1 protein was not retained in the cytoplasm by any of the deletions constructed in the amino acid sequence common to VP-2, suggesting that residues in its unique N-terminal region must drive VP-1 nuclear translocation in a conformation-independent manner. Although not addressed in this work, this end portion of VP-1 possesses basic amino acids clustered in sequences similar to conventional NLSs found in many karyophilic polypeptides (21, 33) that seem to play an active role in VP-1 nuclear transport (70; J. C. Ramírez, E. Lombardo, J. García, and J. M. Almendral, unpublished data). In contrast, VP-2 nuclear transport was halted by deletions created in any part of its sequence. While the activity of some NLSs is highly con-

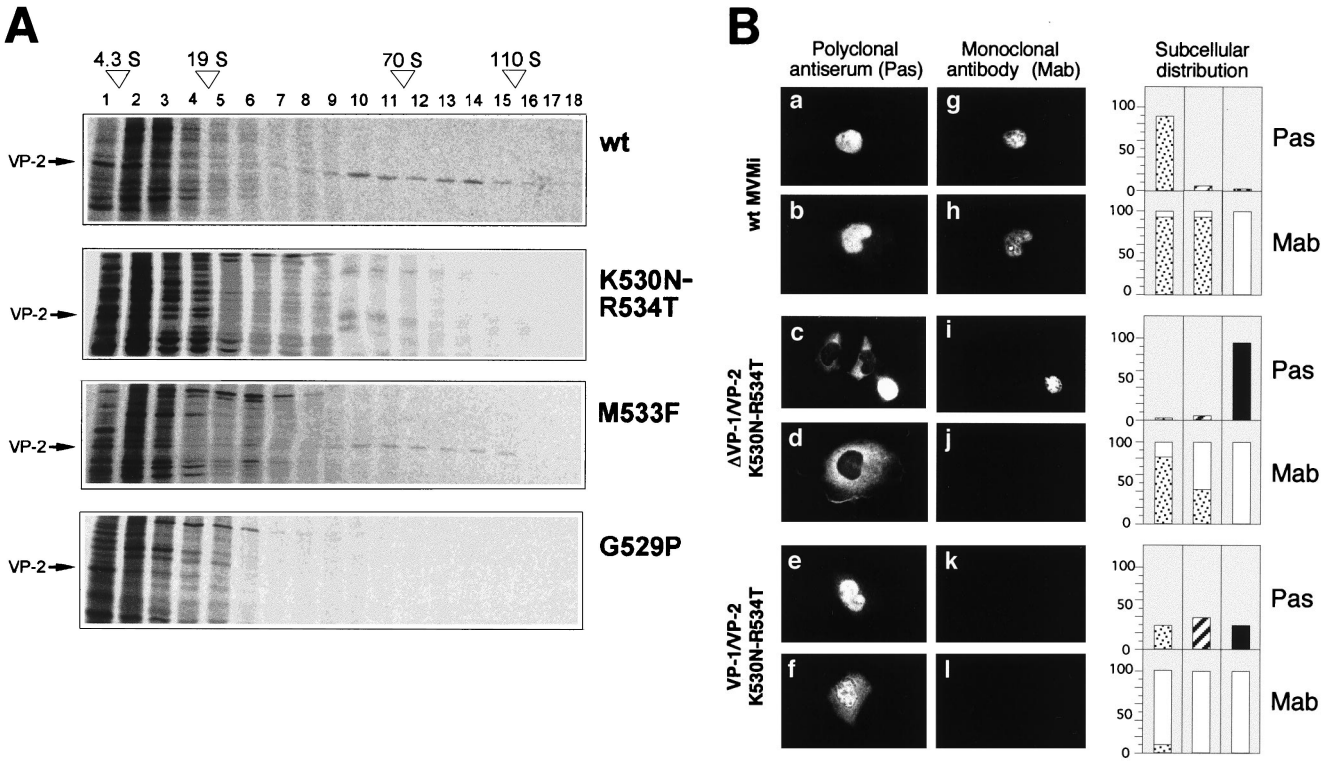

FIG. 3. A functional VP-2 NLM is required for nuclear translocation of VP oligomers and subsequent capsid assembly. (A) Sedimentation analysis of VP-2 mutants. The VP-2 protein mutants indicated on the right labeled with [^{35}S]methionine-[^{35}S]cysteine were subjected to sedimentation through sucrose gradients. Fractions were collected from the top of the tubes, reacted with MVM capsid antiserum, and analyzed by SDS-polyacrylamide gel electrophoresis. Sedimentation profiles of molecular size standards are outlined on the top of the figure. The experiment was repeated twice, with identical results. Gels were overexposed to demonstrate the presence of particles in the 70S to 110S range, and only the sections containing the VP-2 protein are shown. (B) The MVMi capsid assembles in the nucleus. IF of cells transfected with the indicated MVMi plasmids stained with an MVM capsid Pas (panels a to f) and respectively with an anti-capsid specific MAb (panels g to l) is shown. Two different representative examples per each plasmid are shown. The percentages to the right are from >200 cells scored per mutant. Each category of phenotype for the antiserum is subclassified according to the subcellular localization of the MAb reactivity. Stippled bar, nuclear phenotypes; striped bar, mixed phenotypes; black bar, cytoplasmic phenotypes; blank bar, positive cells for the Pas not stained with the MAb.

strained by a particular protein context (20, 52), the extreme sensitivity of VP-2 nuclear transport to any deletion is unusual, an indication that this activity requires the correct cytoplasmic folding of the whole protein and hence its overall conformation. Indeed, wt and mutant VP-2 protein folding in the cytoplasm was verified by their ability to conform capsid epitopes in this compartment, while VP-1 protein appears unable to fold into similar structures (Fig. 1C, mutants Δ60–90 and Δ138–267), another piece of evidence that VP-1 nuclear transport does not require conformational competence of the VP-2 common region.

Cooperative nuclear translocation by VP-1/VP-2 complexing. This study shows that the capsid proteins of parvovirus MVMi interact cooperatively in the cytoplasm in the form of a VP-1 assisted nuclear colocalization of incompetent VP-2 mutants. Examples of this cooperative phenomenon were the IF phenotypes of the ΔVP-1/Δ174–231 and ΔVP-1/Δ323–473 mutants, which had a completely cytoplasmic phenotype for the VP-2 protein (Fig. 1E), while in the presence of VP-1 (Δ174–231 and Δ323–473 mutants), around 40% of the transfected cells showed predominantly VP-2 localized in the nuclear compartment (Fig. 1D).

The coupling of capsid proteins interactions with nuclear transport has also been seen in the parvovirus AAV (55) and other small icosahaedral viruses, as exemplified by the *Polyomavirus* genus (27). The coexpression of the murine polyomavirus VP-1 major capsid protein with the minor capsid proteins VP-2 and VP-3 facilitates their nuclear localization (10, 18), and an interactive determinant was mapped in a C-terminal segment of VP-2/VP-3 that inserts by hydrophobic interactions into the axial cavity of the VP-1 pentamer (13). The fact that cytoplasmic complexes can configure features of the icosahaedral polyomavirus virion is consistent with our observations that structural elements of the mature parvovirus MVMi particle such as the βI strand, capsid epitopes, and VP trimers (see below) are also formed in the cytoplasm of the MVMi-infected cells.

The VP proteins of MVMi deleted between amino acids residues 60 and 127 of VP-2 were not cooperatively transported in the presence of VP-1 (Fig. 1C and D), while mutants deleted between residues 161 and 587 tolerated VP-1/VP-2 cooperative interaction at various levels (Fig. 1D). Thus, although the large deletions created in the VP gene did not allow the precise assignment of the VP-1/VP-2 interactive determinant, the results obtained map amino acids 60 to 161 as an essential region for the cytoplasmic interaction of both proteins. Whether this region contributes to the correct folding of the VP proteins required for their functional interaction or whether it presents a small interactive domain is an important question warranting further research.

Structure and properties of the VP-2 NLM. Protein sequences with nuclear localization capacity are generally rich in basic residues and hydrophilic (38), but no consensus structural motif has been identified. The evidence of a three-dimen-

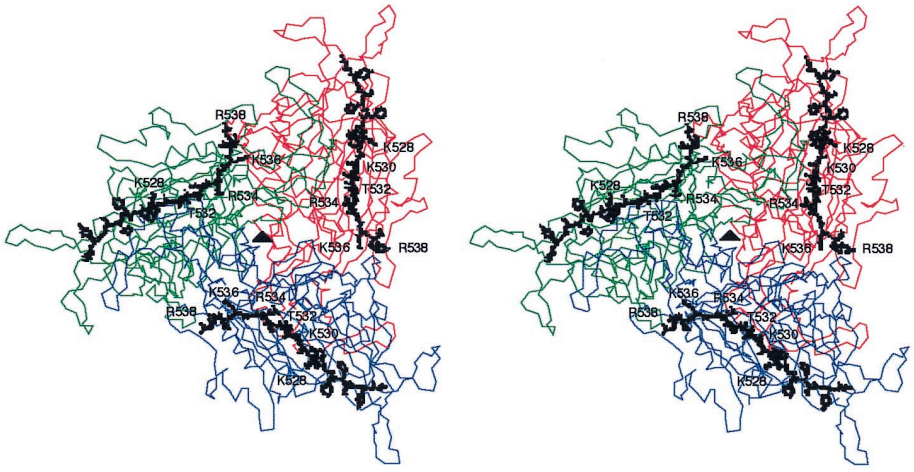

FIG. 4. Structure of an MVMi VP-2 trimer competent for nuclear transport. A stereo diagram of a trimeric MVMi subunit viewed down an icosahedral threefold axis (solid triangle) from the interior of the particle is shown. The figure was generated with the program Molview (64) from available coordinates (PDB accession no. 1MVM). βI is shown in the black ball-and-stick system. Residues in the exposed face of βI involved in the NLM function are labeled.

sional NLM for the MVMi VP-2 capsid protein, shaped at the basic face of the βI, resulted from the consistency of our mutational analysis in both faces of the beta-strand, which showed that its amphipathic nature was required for functionality in nuclear transport (Fig. 2). Computer graphics analysis of mutations further supported that amino acid substitutions hampering the nuclear transport properties of VP-2 are likely to alter the conformation of βI. It is noteworthy that the single G529P mutation that disturbed the natural curvature of the βI completely abrogated its function. This is in contrast to most reported karyophilic protein domains, which commonly have essential proline residues preceding or within their NLS (21, 37, 38, 47), suggesting that most probably they do not work under a beta-strand configuration.

Whether the VP-2 NLM function as a bona fide NLS directly recognizing components of the import machinery or, rather, is required for association with NLS-bearing auxiliary factors (reviewed in reference 30) is a matter that deserves further experiments. The conventional probing of sufficiency for a given NLS, namely, the transfer by peptide insertion of the nuclear translocation capacity to a cytoplasmic polypeptide (32), was unsuccessful with the NLM of VP-2, as could be envisaged since βI must require a certain protein context of interstrand bonding and three-dimensional contacts to adopt its conformation. However, the function of the VP-2 NLM as a nuclear targeting signal is strengthened by the fact that removal of basic residues of βI that led to deficient VP-2 nuclear transport (mutant ΔVP-1/VP-2 K530N-R534T [Fig. 2B]) did not hamper any of the other tested functions of the polypeptide for which an overall protein conformation must also be required, such as oligomerization, cooperative interaction with VP-1, configuration of capsid epitopes, or assembly into capsids in the nucleus (Fig. 1 and 3).

In the sequence alignment of VP-2 from 10 representative parvoviruses evolutionarily related to MVM (12), the amphipathic character of βI, the number of basic residues of the exposed face, and the residues of the hydrophobic face found important for NLM functionality (G529 and L531) are strictly conserved. Thus, an NLM probably mediates the nuclear transport of the major capsid protein in these parvoviruses as well. Computer-assisted searchs of domains with alternate basic residues (and not merely in clusters), combined with structural analyses, may allow the identification of unsuspected NLM in beta-strands of karyophilic polypeptides. Remarkably, some of the conserved basic residues of the NLM of MVMi seem to be involved additionally in interactions with DNA (mutant ΔVP-1/VP-2 K530N-R534 [Fig. 3A]), a property previously described in some NLSs (62, 76). The analysis of the ordered DNA in the canine parvovirus capsid structure (68) showed a low level of specificity associated with the interaction between the DNA bases and the capsid protein, which may contribute to DNA packaging during viral assembly (12). Thus, the mutation in the R534 residue of the NLM may cause a disruption of specific VP-2–DNA interactions necessary for the recognition and encapsidation of the MVMi genome.

The NLM in βI drives VP trimers into the nucleus, contributing to the quality control of viral morphogenesis. Since the stoichiometry of MVM VP-1/VP-2 subunits synthesized in the cytoplasm of the infected cells is 1:5 (17, 56, 58), the efficient VP-1-assisted nuclear localization of around 50% of incompetent VP-2 mutant proteins (Fig. 3B, bottom) cannot be due to a one-to-one VP-1/VP-2 interaction. Rather, this level of cooperativity requires that each VP-1 subunit cotransport oligomerized VP-2 subunits of lower order than pentamers and supports the notion that VP trimers are formed in the cytoplasm prior to nuclear transport. The notion of a VP trimer as a stable precursor in the MVMi assembly pathway is reinforced by the observation that the most extensive interactions in the parvovirus virions occur among the large insertion loops between the βG and βH strands of threefold symmetry-related subunits (74, 75), which intertwine with each other to form the threefold spikes (1, 68). Correspondingly, these intermediates are more stable than either dimers or pentamers, as measured by the buried surface area on oligomer formation (74). Interestingly, in the structure of a VP trimer analyzed apart from the rest of the MVMi capsid (Fig. 4), the basic residues of βI that conform the NLM and confer the nuclear localization capacity to the complex are exposed to solvent and thus accessible to intermolecular interactions.

The NLM and the NLS of VP-1 may play a major regulatory role at several levels of MVMi morphogenesis. As outlined in Fig. 5, these signals should make the following contributions. (i) They should help maintain the stoichiometry. Cytoplasmic trimeric precursors must be translocated at equal rates regard-

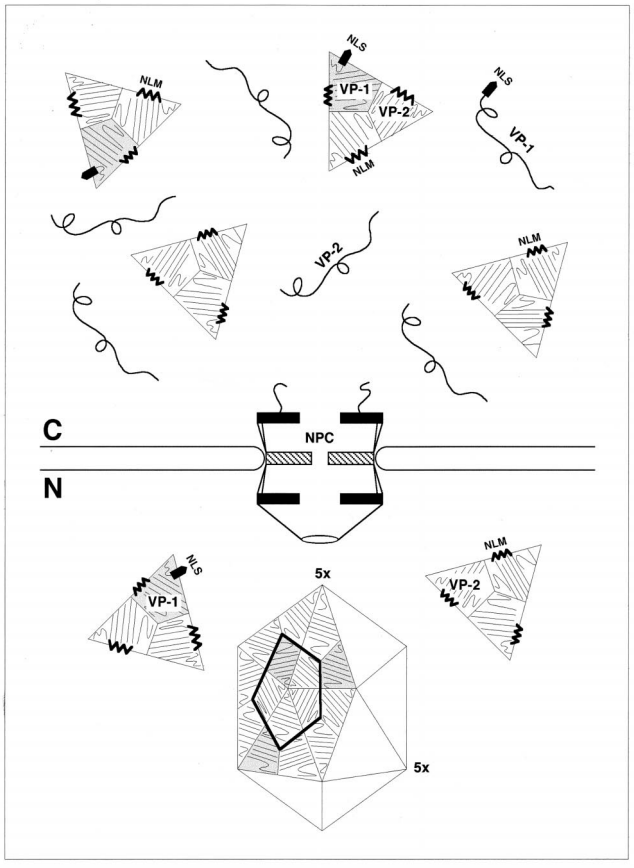

FIG. 5. The role of nuclear transport signalling of capsid proteins in MVMi morphogenesis. C, cytoplasmic events. Viral structural proteins are synthesized at a 1:5 VP-1/VP-2 molar ratio in the infected cell. The subunits interact efficiently, and folding is driven by VP-2 chaperone activity. Two types of trimers are formed without restriction of either VP-2 or VP-1 (shaded) subunits at the stoichiometry of synthesis. These oligomers are equally competent for nuclear translocation by virtue of exposing the configured NLM and the NLS of VP-1 to the nuclear import machinery and the NPC. N, nuclear events. Only correctly folded trimers enter the nucleus and assemble into icosahedral particles. In the mature capsid, the NLS of VP-1 is hidden (16) and the NLM faces to the particle inward (1). Abbreviations: NLS, VP-1 N-terminal 141 amino acids with nuclear localization capacity (70; Ramírez et al., unpublished). 5×, fivefold axis.

less of subunit composition, since an uneven VP-1/VP-2 ratio in the nucleus does not allow stable particle formation (Fig. 3B, bottom). When the NLM is inactivated by genetic mutations, only the VP-1-containing trimer would be competent for nuclear translocation (Fig. 5), accounting for the 50% proportion of VP-2 subunits found in the cytoplasm (Fig. 3B, bottom). (ii) They should help order the morphogenetic flow. The competence for nuclear translocation is acquired only by a precise subviral assembly intermediate, not by unassembled unfolded polypeptides or by an entirely assembled capsid. (iii) They should assist with quality control. Only correctly assembled protein complexes are able to traverse through the NPC, while misfolded polypeptides are excluded from the nucleus, avoiding the impairment of the final morphogenetic steps. Thus, the NPC acts as a narrow and selective window preventing the premature MVMi capsid formation in the cytoplasm.

It is intriguing that although VP-1 and VP-2 have an identical three-dimensional structure in the MVMi particle (1), only VP-2 is able to fold in the cytoplasm (Fig. 1) and to assemble into capsids in the nucleus (Fig. 3) (69). Thus, the driving force leading to VP protein folding must resides in a VP-2 specific chaperone-like activity (Fig. 5, top), which may account for the reported role of VP-2 as the capsid determinant of MVM tropism (39). However, the incompetence of MVMi VP oligomers to assemble into capsids in the cytoplasm, even under high VP protein accumulation (Fig. 3B), suggests that further accessory factors of the nuclear milieu must participate in this highly orchestrated process. Recently, the identification of an NLS in the AAV VP2 protein also suggested that nuclear transport is necessary for capsid formation in this parvovirus (25).

NLMs whose function depends on a correct three-dimensional protein conformation should be susceptible to signals known to modulate NLS activities such as phosphorylation (30), masking (24), or intramolecular conformational changes (61), even when the signals are exerted on physically distant domains, and hence they are advantageous in terms of response to subtle physiological requirements. We are therefore investigating whether the function of the NLM in MVMi capsid proteins contributes to the dependence of the parvovirus life cycle on the host cell proliferative stage (4, 17). It may well be that the morphogenesis of more complex nuclear viruses or the ribosomal biogenesis is similarly regulated at some stages by similar principles, via the configuration of structured NLMs in intermediates of their assembly pathway.

ACKNOWLEDGMENTS

E.L. and J.C.R. contributed equally to this work.

We are indebted to C. Parrish for the kind gift of anti-MVM monoclonal antibodies, to P. Tattersall for providing the MVMi infectious plasmid and for thoughtful interest, to M. G. Rossmann and L. Serrano for their helpful comments, to R. McKenna for critical suggestions on the manuscript, to R. Cuadros for excellent technical assistance, and to all the members of the laboratory for motivating discussions.

This work was supported by grant SAF 98-0019 from the Comisión Interministerial de Ciencia y Tecnología (CICYT) to J.M.A., an institutional grant from Fundación Ramón Areces to the Centro de Biología Molecular Śevero Ochoa," and in part by a Research Development Travel grant from the University of Warwick to M.A.-M. E.L. was supported by a predoctoral fellowship from the Spanish Ministry of Education.

REFERENCES

1. **Agbandje-McKenna, M., A. Llamas-Saiz, F. Wang, P. Tattersall, and M. G. Rossmann.** 1998. Functional implications of the structure of the murine parvovirus minute virus of mice. Structure **6:**1369–1381.
2. **Astell, C. R., M. E. Gardinerd, and P. Tattersall.** 1986. DNA sequence of the lymphotropic variant of minute virus of mice, MVM(i), and comparison with the DNA sequence of the fibrotropic prototype strain. J. Virol. **57:**656–669.
3. **Ball-Goodrich, L. J., and P. Tattersall.** 1992. Two amino acid substitutions within the capsid are coordinately required for acquisition of fibrotropism by the lymphotropic strain of minute virus of mice. J. Virol. **66:**3415–3423.
4. **Berns, K. I.** 1996. Parvoviridae: the viruses and their replication, p. 2173–2197. *In* B. N. Fields (ed.), Virology, 3rd ed. Lippincott-Raven, Philadelphia, Pa.
5. **Bloom, M. E., D. A. Martin, K. L. Oie, M. E. Huhtanen, F. Costello, J. B. Wolfinbarger, S. F. Hayes, and M. Agbandje-McKenna.** 1997. Expression of aleutian mink disease parvovirus capsid proteins in defined segments: localization of immunoreactive sites and neutralizing epitopes to specific regions. J. Virol. **71:**705–714.
6. **Boissy, R., and C. R. Astell.** 1985. An *Escherichia coli recBC sbc BrecF* host permits the deletion-resistant propagation of plasmid clones containing the 5′-terminal palindrome of minute virus of mice. Gene **35:**179–185.
7. **Bonnard, G. D., E. K. Manders, D. A. Campbell, R. B. Herberman, and M. J. Collins.** 1976. Immunosuppressive activity of a subline of the mouse EL-4 lymphoma. J. Exp. Med. **143:**187–205.
8. **Bordo, D., and P. Argos.** 1991. Suggestions for "safe" residue substitutions in site-directed mutagenesis. J. Mol. Biol. **217:**721–729.
9. **Brownstein, D. G., A. L. Smith, R. O. Jacoby, E. A. Johnson, G. Hansen, and P. Tattersall.** 1991. Pathogenesis of infection with a virulent allotropic variant of minute virus of mice and regulation by host genotype. Lab. Investig. **65:**357–363.
10. **Cai, X., D. Chang, S. Rottinghaus, and R. A. Consigili.** 1994. Expression and

purification of recombinant polyomavirus VP2 protein and its interactions with polyomavirus proteins. J. Virol. **68:**7609–7613.
11. **Chapman, M. S., and M. C. Rossman.** 1993. Structure, sequence, and function correlations among parvoviruses. Virology **194:**491–508.
12. **Chapman, M. S., and M. C. Rossman.** 1995. Single-stranded DNA-protein interactions in canine parvovirus. Structure **3:**151–162.
13. **Chen, X. S., T. Stehle, and S. C. Harrison.** 1998. Interaction of polyomavirus internal protein VP2 with the major capsid protein VP1 and implications for participation of VP2 in viral entry. EMBO J. **17:**3233–3240.
14. **Cingolani, G., C. Petosa, K. Weis, and C. W. Müller.** 1999. Structure of importin-β bound to the IBB domain of importin-α. Nature **399:**221–229.
15. **Conti, E., M. Uy, L. Leighton, G. Blobel, and J. Kuriyan.** 1998. Crystallographic analysis of the recognition of a nuclear localization signal by the nuclear import factor karyopherin α. Cell **94:**193–204.
16. **Cotmore, S. F., A. M. D'Abramo, M. T. Christine, and P. Tattersall.** 1999. Controlled conformational transitions in the MVM virions expose the VP-1 N-terminus and viral genome without particle disassembly. Virology **254:** 169–181.
17. **Cotmore, S. F., and P. Tattersall.** 1987. The autonomously replicating parvoviruses of vertebrates. Adv. Virus Res. **33:**91–173.
18. **Delos, S. E., L. Montross, R. B. Moreland, and R. L. Garcea.** 1993. Expression of the polyomavirus VP2 and VP3 proteins in insect cells: coexpression with the major capsid protein VP1 alters VP2/VP3 subcellular localization. Virology **194:**393–398.
19. **Feldherr, C. M., E. Kallenbach, and N. Schultz.** 1984. Movement of a karyophilic protein through the nuclear pore of oocytes. J. Cell Biol. **99:** 2216–2222.
20. **Gao, M., and D. M. Knipe.** 1992. Distal protein sequences can affect the function of a nuclear localization signal. Mol. Cell. Biol. **12:**1330–1339.
21. **García-Bustos, J., J. Heitman, and M. N. Hall.** 1991. Nuclear protein localization. Biochim. Biophys. Acta **1071:**83–101.
22. **Gardiner, E. M., and P. Tattersall.** 1988. Evidence that developmentally regulated control of gene expression by a parvoviral allotropic determinant is particle mediated. J. Virol. **62:**1713–1722.
23. **Harlow, E., and D. Lane.** 1988. Antibodies: a laboratory manual. Cold Spring Harbor Laboratory, Cold Spring Harbor, N.Y.
24. **Henkel, T., V. Zabel, K. van Zee, J. M. Müller, E. Fanning, and P. A. Baeuerle.** 1992. Intramolecular masking of the nuclear location signal and dimerization domain in the precursor for the p50 NF-κB subunit. Cell **68:** 1121–1133.
25. **Hoque, M., K.-I. Ishizu, A. Matsumoto, S.-I. Han, F. Arisaka, M. Takayama, K. Suzuki, K. Kato, T. Kanda, H. Watanabe, and H. Handa.** 1999. Nuclear transport of the major capsid protein is essential for adeno-associated virus capsid formation. J. Virol. **73:**7912–7915.
26. **Hunter, L. A., and R. J. Samulski.** 1992. Colocalization of adeno-associated virus rep and capsid proteins in the nuclei of infected cells. J. Virol. **66:**317–324.
27. **Ishii, N., A. Nakanishi, M. Yamada, M. H. Macalalad, and H. Kasamatsu.** 1994. Functional complementation of nuclear targeting-detective mutants of simian virus 40 structural proteins. J. Virol. **68:**8209–8216.
28. **Izaurralde, E., M. Kann, N. Panté, B. Sodeik, and T. Hohn.** 1999. Viruses, microorganisms and scientists meet the nuclear pore. EMBO J. **18:**289–296.
29. **Jäkel, S., and D. Görlih.** 1998. Importin β, transportin, RanBP5 and RanBP7 mediate nuclear import of ribosomal proteins in mammalian cells. EMBO J. **17:**4491–4502.
30. **Jans, D. A., and S. Hübner.** 1996. Regulation of protein transport to the nucleus: central role of phosphorylation. Phys. Rev. **76:**651–685.
31. **Jones, T. A., J.-Y. Zou, S. W. Cowan, and M. Kjeldgaard.** 1991. Improved methods for building protein models in electron-density maps and the location of errors in these models. Acta Crystallogr. **A47:**110–119.
32. **Kalderon, D., B. L. Roberts, W. D. Richardson, and A. E. Smith.** 1984. A short amino acid sequence able to specify nuclear location. Cell **39:**499–509.
33. **Kalderon, D., W. D. Richardson, A. F. Markham, and A. E. Smith.** 1984. Sequence requirements for nuclear location of simian virus 40 large-T antigen. Nature **311:**33–38.
34. **Kann, M., B. Sodeik, A. Vlachou, W. H. Gerlich, and A. Helenius.** 1999. Phosphorylation-dependent binding of hepatitis B virus core particles to the nuclear pore complex. J. Cell Biol. **145:**45–55.
35. **Kasmatsu, H., and A. Nakanishi.** 1998. How do animal DNA viruses get to the nucleus? Annu. Rev. Microbiol. **52:**627–686.
36. **Kunkel, A. K.** 1985. Rapid and efficient site-specific mutagenesis without phenotypic selection. Proc. Natl. Acad. Sci. USA **82:**488–492.
37. **Makkerh, J. P. S., C. Dingwall, and R. A. Laskey.** 1996. Comparative mutagenesis of nuclear localization signals reveals the importance of neutral and acidic amino acids. Curr. Biol. **6:**1025–1027.
38. **Mattaj, I. W., and L. Englmeier.** 1998. Nucleocytoplasmic transport: the soluble phase. Annu. Rev. Biochem. **67:**265–306.
39. **Maxwell, I. H., A. L. Spitzer, F. Maxwell, and D. J. Pintel.** 1995. The capsid determinant of fibrotropism for the MVMp strain of minute virus of mice functions via VP2 and not VP1. J. Virol. **69:**5829–5832.
40. **Michael, W. M., P. S. Eder, and G. Dreyfuss.** 1997. The nuclear shuttling domain: a novel signal for nuclear import and nuclear export in the hnRNP K protein. EMBO J. **16:**3587–3598.
41. **Minor, D. L., and P. S. Kim.** 1994. Measurement of the β-sheet-forming propensities of amino acids. Nature **367:**660–663.
42. **Nigg, E. A.** 1997. Nucleocytoplasmic transport: signals, mechanisms and regulation. Nature **386:**779–787.
43. **Palmeri, D., and M. H. Malim.** 1999. Importin β can mediate the nuclear import of an arginine-rich nuclear localization signal in the absence of importin α. Mol. Cell. Biol. **19:**1218–1225.
44. **Parrish, C. R., and L. E. Carmichael.** 1986. Characterization and recombination mapping of an antigenic and host range mutation of canine parvovirus. Virology **148:**121–132.
45. **Parrish, C. R., C. F. Aquadro, M. L. Strassheim, J. F. Evermann, J.-Y. Sgro, and H. O. Mohammed.** 1991. Rapid antigenic-type replacement and DNA sequence evolution of canine parvovirus. J. Virol. **65:**6544–6552.
46. **Pemberton, L. F., G. Blobel, and S. Rosenblum.** 1998. Transport routes through the nuclear pore complex. Curr. Opin. Cell Biol. **10:**392–399.
47. **Pollard, V. W., W. M. Michael, S. Nakielny, M. C. Siomi, F. Wang, and G. Dreyfuss.** 1996. A novel receptor-mediated nuclear protein import pathway. Cell **86:**985–994.
48. **Popov, S., M. Rexach, G. Zybarth, N. Reiling, M.-A. Lee, L. Ratner, C. M. Lane, M. S. Moore, G. Blobel, and M. Bukrinsky.** 1998. Viral protein R regulates nuclear import of the HIV-1 pre-integration complex. EMBO J. **17:**909–917.
49. **Ramírez, J. C., A. Fairén, and J. M. Almendral.** 1996. Parvovirus minute virus of mice strain i multiplication and pathogenesis in the newborn mouse brain is restricted to proliferative areas and to migratory cerebellar young neurons. J. Virol. **70:**8109–8116.
50. **Ribbeck, K., G. Lipowsky, H. M. Kent, M. Stewart, and D. Görlich.** 1998. NTF2 mediates nuclear import of Ran. EMBO J. **17:**6587–6598.
51. **Robbins, J., S. M. Dilworth, R. A. Laskey, and C. Dingwall.** 1991. Two interdependent basic domains in nucleoplasmin nuclear targeting sequence: identification of a class of bipartite nuclear targeting sequence. Cell **64:**651–623.
52. **Roberts, B. L., W. D. Richardson, and A. E. Smith.** 1987. The effect of protein context on nuclear location signal function. Cell **50:**465–475.
53. **Rossmann, M. G., and J. E. Johnson.** 1989. Icosahaedral RNA virus structure. Annu. Rev. Biochem. **58:**433–573.
54. **Rout, M. P., G. Blobel, and J. D. Aitchison.** 1997. A distinct nuclear import pathway used by ribosomal proteins. Cell **89:**715–725.
55. **Ruffing, M., H. Zentgraf, and J. A. Kleinschmidt.** 1992. Assembly of virus like particles by recombinant structural proteins of adeno-associated virus type 2 in insect cells. J. Virol. **66:**6922–6930.
56. **Santarén, J. F., J. C. Ramírez, and J. M. Almendral.** 1993. Protein species of the parvovirus Minute Virus of Mice strain MVMp: involvement of phosphorylated VP-2 subtypes in viral morphogenesis. J. Virol. **67:**5126–5138.
57. **Schaap, P. J., J. V. Riet, C. L. Woldringh, and H. A. Raué.** 1991. Identification and functional analysis of the nuclear localization signals of ribosomal protein L25 from *Saccharomyces cerevisiae*. J. Mol. Biol. **221:**225–237.
58. **Schoborg, R. V., and D. Pintel.** 1991. Accumulation of MVM gene products is differentially regulated by transcription initiation, RNA processing and protein stability. Virology **181:**22–34.
59. **Segovia, J. C., J. M. Gallego, J. A. Bueren, and J. M. Almendral.** 1999. Severe leukopenia and dysregulated erythropoiesis in SCID mice persistently infected by the parvovirus minute virus of mice. J. Virol. **73:**1774–1784.
60. **Shah, S., S. Tugendreich, and D. Forbes.** 1998. Major binding sites for the nuclear import receptor are the integral nucleoporin Nup153 and the adjacent nuclear filament protein Tpr. J. Cell Biol. **141:**31–49.
61. **Sheldon, L. A., and R. E. Kingston.** 1993. Hydrophobic coiled-coil domains regulate the subcellular localization of human heat shock factor 2. Genes Dev. **7:**1549–1558.
62. **Skiadopoulos, M. H., and A. McBride.** 1996. The bovine papillomavirus type 1 E2 transactivator and repressor proteins use different nuclear localization signals. J. Virol. **70:**1117–1124.
63. **Smith, C. K., and L. Reagan.** 1995. Guidelines for protein design: the energetics of β sheets side chain interactions. Science **270:**980–982.
64. **Smith, T. J.** 1990. MacInPlot: a program to display electron density and atomic models on the Macintosh personal computer. J. Appl. Crystallogr. **23:**141–142.
65. **Stoffler, D., B. Fahrenkrog, and U. Aebi.** 1999. The nuclear pore complex: from molecular architecture to functional dynamics. Curr. Opin. Cell Biol. **11:**391–401.
66. **Tattersall, P., A. J. Shatkin, and D. C. Ward.** 1977. Sequence homology between the structural polypeptides of minute virus of mice. J. Mol. Biol. **111:**375–394.
67. **Taylor, W. R.** 1986. The classification of amino acid conservation. J. Theor. Biol. **119:**205–218.
68. **Tsao, J., M. S. Chapman, M. Agbandje, W. Keller, K. Smith, H. Wu, M. Luo, T. J. Smith, M. G. Rossmann, R. W. Compans, and C. R. Parrish.** 1991. The three-dimensional structure of canine parvovirus and its functional implications. Science **251:**1456–1464.

69. **Tullis, G. E., R. B. Lisa, and D. J. Pintel.** 1993. The minor capsid protein VP1 of the autonomous parvovirus minute virus of mice is dispensable for encapsidation of progeny single-stranded DNA but is required for infectivity. J. Virol. **67:**131–141.
70. **Vihinen-Ranta, M., L. Kakkola, A. Kakela, P. Vilja, and M. Vuento.** 1997. Characterization of a nuclear localization signal of canine parvovirus capsid proteins. Eur. J. Biochem. **250:**389–394.
71. **Vodicka, M. A., D. M. Koepp, P. A. Silver, and M. Emermann.** 1998. HIV-1 Vpr interacts with the nuclear transport pathway to promote macrophage infection. Genes Dev. **12:**175–185.
72. **Wang, P., P. Palese, and R. E. O'Neill.** 1997. The NPI-1/NPI-3 (karyopherin α) binding site on the influenza A virus nucleoprotein NP is a nonconventional nuclear localization signal. J. Virol. **71:**1850–1856.
73. **Wistuba, A., A. Kern, S. Weger, D. Grimm, and J. A. Kleinschmidt.** 1997. Subcellular compartmentalization of adeno-associated virus type 2 assembly. J. Virol. **71:**1341–1352.
74. **Wu, H., and M. C. Rossmann.** 1993. The canine parvovirus empty capsid structure. J. Mol. Biol. **233:**231–244.
75. **Xie, Q., and M. S. Chapman.** 1996. Canine parvovirus capsid structure analyzed at 2.9 Å resolution. J. Mol. Biol. **264:**497–520.
76. **Zandi, E., T.-N. T. Tran, W. Chamberlain, and C. S. Parker.** 1997. Nuclear entry, oligomerization, and DNA binding of the *Drosophila* heat shock transcription factor are regulated by a unique nuclear localization sequence. Genes Dev. **11:**1299–1314.